

# JND-Guided Light-Weight Neural Pre-Filter for Perceptual Image Coding

<sup>1</sup>Chenlong He <sup>†</sup>, <sup>1</sup>Zijing Dong <sup>†</sup>, <sup>1</sup>Min Li, <sup>2</sup>Zhijian Hao, <sup>3</sup>Leilei Huang <sup>\*</sup>, <sup>1</sup>Xiaoyang Zeng <sup>Member, IEEE</sup>,  
and <sup>1</sup>Yibo Fan <sup>\* Member, IEEE</sup>

<sup>1</sup>Fudan University, Shanghai <sup>2</sup>Xidian University, Xi'an <sup>3</sup>East China Normal University, Shanghai  
<sup>1</sup>clhe22@m.fudan.edu.cn <sup>1</sup>fanyibo@fudan.edu.cn, <sup>3</sup>llhuang@cee.ecnu.edu.cn

**Abstract**— Just Noticeable Distortion (JND)-guided pre-filter is a promising technique for improving the perceptual compression efficiency of image coding. However, existing methods are often computationally expensive, and the field lacks standardized benchmarks for fair comparison. To address these challenges, this paper introduces a twofold contribution. First, we develop and open-source *FJNDF-Pytorch*, a unified benchmark for Frequency-domain JND-Guided pre-Filters. Second, leveraging this benchmark, we propose a complete learning framework for a novel, lightweight Convolutional Neural Network (CNN). Experimental results demonstrate that our proposed method achieves better compression efficiency, consistently outperforming existing approaches across multiple datasets and encoders. In terms of computational cost, our model is exceptionally lightweight, requiring only 7.15 GFLOPs to process a 1080p image, which is merely 14.1% of the cost of a leading lightweight network in the field. Our work presents a robust solution that demonstrates superior performance and efficiency, supported by a reproducible research platform. The implementation is available at <https://github.com/viplab-fudan/FJNDF-Pytorch>.

**Index Terms**—Perceptual Coding, Just Notice Distortion, Pre-Filter, Neural Network

## I. INTRODUCTION

Enhancing the compression efficiency of encoders based on perceptual quality is a core challenge in perceptual coding. Among the various techniques, pre-filter guided by Just Noticeable Distortion (JND) has become a promising approach due to its portability as an encoder-only modification. Existing methods [1]–[9] can be broadly categorized by the type of JND model employed: spatial domain [1]–[3], frequency domain [4]–[6], hybrid spatial-frequency domain [7], and learning-based models [8], [9].

However, current research in this area suffers from two key limitations: 1) the majority of studies rely on Mean Opinion Score (MOS) for video quality evaluation, a metric that is time-consuming and labor-intensive, thereby hindering rapid algorithm iteration and large-scale validation; 2) many works generally fail to employ the Bjøntegaard Delta Bitrate (BD-BR) [10] to evaluate their impact on compression performance, thus lacking an objective quantification of efficiency gains.

While the few studies [5], [6] that utilize BD-BR confirm that traditional frequency-domain methods are effective, they suffer from prohibitive computational complexity. Their

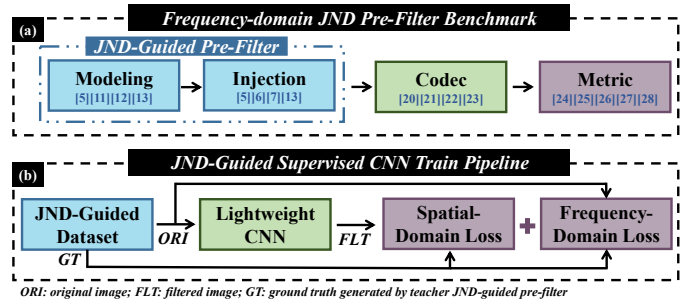


Fig. 1. Illustration of our main contributions. (a) We build a standardized benchmark for frequency-domain JND pre-filters. (b) Using this benchmark, we generate a dataset to train our proposed lightweight CNN via a supervised pipeline, which is optimized by a joint spatial and frequency loss function.

reliance on expensive operations like the Discrete Cosine Transform (DCT) and additional detail enhancement modules for salient regions results in a severe increase in encoding time, with overheads reaching up to 313% [5] and 123% [6].

In summary, current research on JND-guided pre-filter faces two primary challenges: a **limited evaluation methodology**, which relies on subjective metrics and lacks standardized benchmarks for objective comparison, and the **high complexity of advanced algorithms**, which renders the most effective frequency-domain methods impractical for real-time application. This paper addresses these gaps with two main contributions, as illustrated in Fig. 1:

- We develop and open-source **FJNDF-Pytorch**, a unified platform for the development and validation of JND pre-filter methods. The platform integrates: 1) mainstream frequency-domain JND modeling and injection methods; 2) multiple standard open-source encoders and datasets; 3) a suite of objective quality metrics, to facilitate reproducible research and address the evaluation gap.
- We propose a **complete framework for lightweight neural pre-filter**. Leveraging our benchmark to generate a high-quality dataset, the framework then effectively trains a lightweight network to learn the fundamental characteristics of the reference filter via a supervised, residual learning strategy. The core of our method is a novel hybrid loss function, featuring a frequency-domain loss, which then empowers the network to surpass the performance of this training reference.

<sup>†</sup>These authors contributed equally to this work.

<sup>\*</sup>Corresponding author.

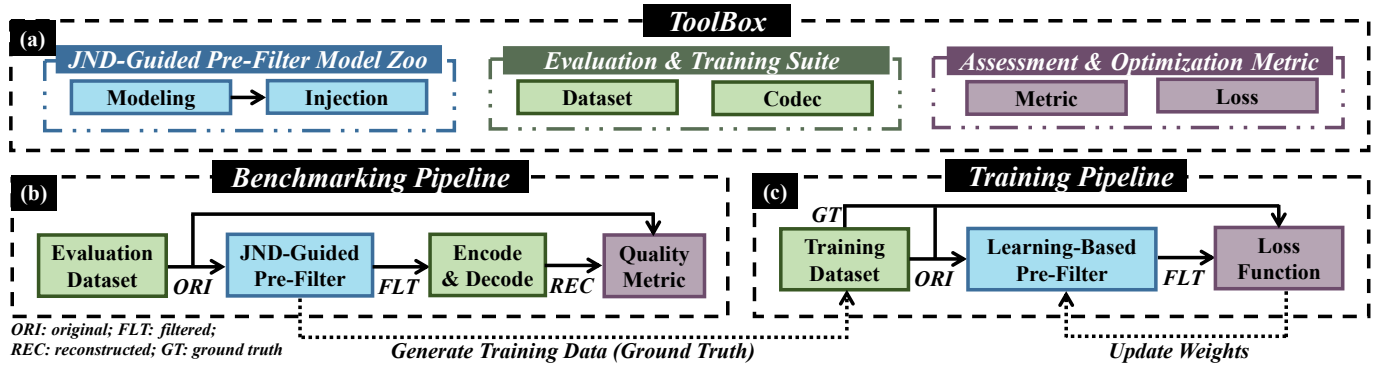


Fig. 2. An overview of the FJNDF-Pytorch framework. (a) The modular toolbox, whose components are detailed in Table I, supports two primary pipelines. (b) A benchmarking pipeline for evaluating filters and generating training data. (c) A training pipeline that leverages this data to train learning-based pre-filters.

TABLE I  
COMPONENTS INTEGRATED IN THE FJNDF-PYTORCH TOOLBOX

Module	Integrated Components
<b>JND-Guided Pre-Filter Model Zoo</b>	
Modeling	Mainstream DCT-domain models [5], [11]–[13]
Injection	Mainstream injection methods [5]–[7], [13]
<b>Evaluation &amp; Training Suite</b>	
Dataset	<b>Evaluation:</b> HEVC-B [14], XIPH [15], MCL-JCV [16], MCL-JCI [17] <b>Training:</b> DIV2K [18], KonJND-1K [19]
Codec	x264 [20], x265 [21], libaom [22], VVenC [23] (+ decoders)
<b>Assessment &amp; Optimization Metric</b>	
Metric	PSNR, PSNR-HVSM [24], SSIM [25], MS-SSIM [26], VMAF [27], VMAF-NEG [28]
Loss	L1, L2, Charbonnier [29], MS-SSIM [30] Loss

## II. THE FJNDF-PYTORCH BENCHMARK

The architecture of our FJNDF-Pytorch framework is illustrated in Fig. 2. Inspired by established platforms such as IQA-Pytorch [31] and BasicSR [32], our benchmark is designed to power a complete research pipeline, from algorithm benchmarking to model training. Due to space constraints, this section focuses on the core components of the JND-guided pre-filter: the **Modeling** and **Injection** stages.

### A. JND Modeling

The principle of JND modeling is to quantify the maximum distortion that falls below the perception threshold of Human Visual System (HVS). This is typically achieved via a multiplicative fusion model that estimates a JND threshold  $J_T$ , by integrating key HVS effects, as shown in Eq. (1):

$$J_T(u, v, N) = s \cdot J_{CSF} \cdot J_{LA} \cdot J_{CM} \cdot J_{SA}, \quad (1)$$

where  $(u, v)$  are the frequency coordinates within an  $N \times N$  DCT block, and  $s$  is the summation effect factor. The terms  $J_{CSF}$ ,  $J_{LA}$ ,  $J_{CM}$ , and  $J_{SA}$  represent the perceptual effects of the Contrast Sensitivity Function (CSF), Luminance Adaptation (LA), Contrast Masking (CM), and Saliency Adaptation (SA).

Our benchmark integrates four representative JND models [5], [11]–[13] to cover the field’s breadth and depth. **For breadth**, we include models [11] and [12], which represent two distinct paradigms for CSF and LA modeling. **For depth**,

TABLE II  
RESULTS OF THE TOP-THREE PERFORMING ALGORITHMS ON VVENC

Dataset	Method $M^a + I^b$	PSNR	PSNR-HVSM	MS-SSIM	VMAF-NEG	ALL
HEVC-B [14]	[5] + [6]	<b>1.94</b>	-2.83	-1.36	<b>-0.86</b>	<b>-0.78</b>
	[13] + [6]	1.95	-2.75	-1.35	-0.67	-0.70
	[5] + [7]	4.91	<b>-4.29</b>	<b>-2.04</b>	-0.85	-0.57
XIPH [15]	[12] + [7]	-0.27	<b>-4.17</b>	-2.76	<b>-2.87</b>	<b>-2.52</b>
	[13] + [6]	<b>-0.45</b>	-3.95	<b>-3.14</b>	-2.53	-2.52
	[5] + [6]	-0.44	-3.98	-3.07	-2.54	-2.51
MCL-JCV [16]	[13] + [6]	0.32	-2.57	<b>-2.07</b>	<b>-1.50</b>	<b>-1.46</b>
	[5] + [6]	<b>0.31</b>	<b>-2.64</b>	-2.05	-1.43	-1.45
	[12] + [7]	0.49	<b>-2.64</b>	-1.35	-1.31	-1.20
MCL-JCI [17]	[12] + [13]	<b>8.52</b>	<b>-11.11</b>	<b>-5.34</b>	-4.00	<b>-2.99</b>
	[5] + [7]	8.84	-10.39	-4.63	<b>-4.85</b>	-2.76
	[13] + [7]	8.79	-10.29	-4.46	-4.54	-2.63

<sup>a</sup> $M$  and <sup>b</sup> $I$  denotes the method for JND Modeling and Injection, respectively

we include model [13] (which adds CM to [12]) and model [5] (which adds SA to [13]), forming a clear evolutionary path.

### B. JND Injection

JND injection translates the computed threshold  $J_T$  into signal modifications to remove perceptual redundancy. The integrated methods can be categorized into two main strategies. The first, **Coefficient Suppression**, directly reduces the magnitude of DCT coefficients ( $C_o$ ). This includes a range of methods, from basic suppression [13] to more sophisticated approaches. Frequency-weighted suppression [7] introduces a suppression weight  $p$  that is dependent on  $(u, v)$ , and [6] further condition this weight on the block type  $B$ . This progressive refinement is generalized by the formula in Eq. (2):

$$C_f = \begin{cases} \text{sgn}(C_o) \cdot \sqrt{C_o^2 - p(u, v, B) \cdot J_T^2}, & \text{else} \\ 0, & \text{if } |C_o| < J_T \end{cases} \quad (2)$$

The second strategy, a **Filter Approach** [5], implements injection through a low-pass Gaussian filter whose variance is controlled by  $J_T$ .

Leveraging this benchmark, we conduct a comprehensive evaluation by testing all combinations of the integrated JND modeling and injection methods. To provide a clear summary of the most effective strategies, we report the top-three performing combinations for each dataset on VVenC in Table II.

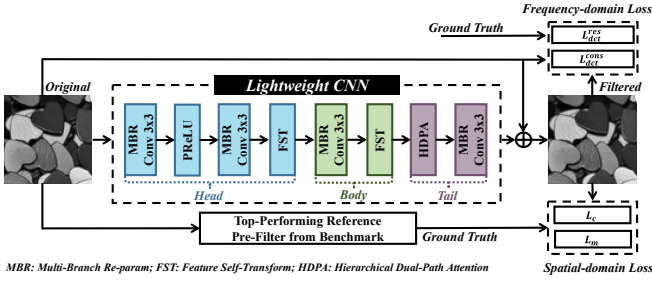


Fig. 3. Training pipeline of our lightweight pre-filter network. Our core contribution, the hybrid loss, supervises the network. The spatial-domain loss ( $L_c, L_m$ ) is computed against a Ground Truth (GT) from a reference filter. The frequency-domain loss imposes a residual constraint ( $L_{dct}^{res}$ ) against the GT and a conservation constraint ( $L_{dct}^{cons}$ ) against the original input. The network backbone (MBR, FST and HDPA) is detailed in [33]. MBR is re-parameterized into standard convolutions at inference pipeline.

### III. JND-GUIDED LIGHTWEIGHT NETWORK

Our proposed method is a complete learning framework designed to train a lightweight network for JND-guided pre-filter. As illustrated in Fig. 3, we employ a supervised learning paradigm with a residual learning strategy, which reduces the task’s complexity and makes it feasible for a lightweight network. The framework is composed of three key components: a hybrid loss function designed to enable the network to surpass the performance of its reference, a data generation strategy to provide a high-quality training target, and a customized lightweight network architecture for efficient inference.

#### A. Hybrid Loss Function Design

To enable the network to surpass the performance of the traditional reference algorithm, the core of our methodology is a hybrid loss function that incorporates frequency-domain priors. The total loss,  $L_{all}$ , is a weighted sum of a spatial-domain loss and our proposed frequency-domain loss,  $L_{freq}$ :

$$L_{all} = \lambda_1 L_c(I_f, I_{gt}) + \lambda_2 L_m(I_f, I_{gt}) + \lambda_3 L_{freq}(C_f, C_{gt}, C_o) \quad (3)$$

The spatial-domain loss, guides the network to learn the fundamental behavior of the reference algorithm. As shown in the lower path of Fig. 3, it is computed between the network’s filtered output ( $I_f$ ) and the GT ( $I_{gt}$ ) generated by the reference pre-filter. It consists of a Charbonnier [29] loss ( $L_c$ ) for pixel-level fidelity and an MS-SSIM [30] loss ( $L_m$ ) for multi-scale structural similarity.

Our key innovation is the frequency-domain loss,  $L_{freq}$ , which combines a reference-dependent distillation term with reference-independent physical constraints, allowing the network to correct the flaws of its training target. It is composed of two terms:

$$L_{freq} = L_{dct}^{res} + L_{dct}^{cons} \quad (4)$$

The first term, the *Frequency-Domain Residual Loss* ( $L_{dct}^{res}$ ), serves as a distillation constraint. It penalizes the energy of the residual between the DCT coefficients of  $I_f$  and  $I_{gt}$ , promoting a deeper learning of the reference’s behavior in the frequency domain and is formulated as:

$$L_{dct}^{res} = \sum_{u,v} (C_f - C_{gt})^2 \quad (5)$$

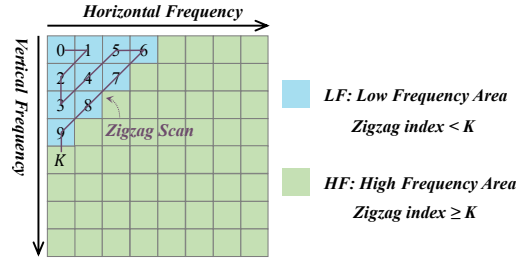


Fig. 4. Illustration of the frequency area partitioning for our proposed conservation constraint loss,  $L_{dct}^{cons}$ . An 8x8 DCT block is divided into a Low-Frequency ( $LF$ ) and a High-Frequency ( $HF$ ) area based on a zigzag scan order and a predefined threshold,  $K$ .

The second term is the *Frequency Conservation Constraint Loss* ( $L_{dct}^{cons}$ ), which references the original input ( $I_o$ ) to enforce physical plausibility. As illustrated in Fig. 4, this loss partitions the 8x8 DCT block into Low-Frequency ( $LF$ ) and High-Frequency ( $HF$ ) areas. It then imposes a bidirectional, asymmetric constraint:

$$L_{dct}^{cons} = \sum_{(u,v) \in LF} \max(0, |C_o| - |C_f|)^2 + \sum_{(u,v) \in HF} \max(0, |C_f| - |C_o|)^2 \quad (6)$$

The  $LF$  term prevents over-smoothing by penalizing the loss of low-frequency energy, while the  $HF$  term suppresses artifacts by penalizing the creation of new high-frequency energy. This constraint empowers the network to surpass the reference by correcting its frequency-domain imperfections.

#### B. Data Generation Strategy

To generate the training data, we adopt a data-driven approach. Leveraging our benchmark, we select the top-performing traditional pre-filter, [13] + [6], from Table II as the reference algorithm to process the DIV2K [18] and KonJND-1K [19] datasets, creating 2,008 original-reference image pairs, providing a validated, high-quality learning target for subsequent network training.

#### C. Lightweight Network Architecture

We select the efficient MobileNetIE [33] as our backbone, leveraging its re-parameterization mechanism for low inference complexity. To further specialize this general-purpose model for our JND-Guided pre-filter task, we introduce two key architectural modifications. **First**, we replace all 5x5 convolutions with 3x3 to better align the network’s receptive field with the local nature of DCT-domain operations. **Second**, we design a bottleneck-expansion channel configuration, as illustrated by the *Head*, *Body*, and *Tail* structure in Fig. 3.

Specifically, while the backbone maintains a relatively uniform channel width across its stages, we narrow the channels in the *Head* and *Body* before expanding them in the *Tail*. This structure encourages the network to learn a compact and refined feature representation in the early layers, enhancing parameter efficiency. These customizations yield an 41% reduction in computational cost over the backbone, resulting in a highly specialized and efficient model.

TABLE III  
PERFORMANCE COMPARISON OF DIFFERENT PRE-FILTER METHODS ACROSS VARIOUS DATASETS ON VVENC.

Dataset	PSNR				PSNR-HVSM				SSIM				MS-SSIM				VMAF				VMAF-NEG				ALL			
	[5]	[6]	[9]	Ours	[5]	[6]	[9]	Ours	[5]	[6]	[9]	Ours	[5]	[6]	[9]	Ours	[5]	[6]	[9]	Ours	[5]	[6]	[9]	Ours	[5]	[6]	[9]	Ours
HEVC-B	1.55	1.95	1.51	<b>0.87</b>	-1.81	-2.75	-2.53	<b>-4.20</b>	1.84	-0.73	-1.78	<b>-2.05</b>	-0.79	-1.35	-2.34	<b>-2.90</b>	1.50	-0.54	-2.42	<b>-4.84</b>	0.03	-0.67	-1.81	<b>-3.67</b>	0.39	-0.68	-1.56	<b>-2.80</b>
XIPH	-0.77	-0.45	-0.31	<b>-1.16</b>	-3.15	-3.95	-3.07	<b>-5.32</b>	0.82	-2.15	-1.98	<b>-2.78</b>	-1.66	-3.14	-2.78	<b>-4.13</b>	0.09	-2.55	-4.12	<b>-6.26</b>	-1.31	-2.53	-3.27	<b>-5.07</b>	-1.00	-2.46	-2.59	<b>-4.12</b>
MCL-JCV	0.45	0.32	0.21	<b>-0.26</b>	-2.00	-2.57	-1.94	<b>-3.64</b>	1.02	-1.21	-1.30	<b>-1.73</b>	-1.33	-2.07	-1.88	<b>-2.69</b>	1.58	-1.38	-2.72	<b>-5.05</b>	0.21	-1.50	-2.12	<b>-3.61</b>	-0.01	-1.40	-1.63	<b>-2.83</b>
MCL-JCI	2.81	4.81	3.73	<b>2.74</b>	-6.49	-6.31	-7.51	<b>-8.80</b>	3.01	-0.17	-2.04	<b>-2.20</b>	-3.20	-2.77	-5.57	<b>-5.98</b>	-0.91	-2.58	-5.62	<b>-7.55</b>	-2.66	-2.77	-4.88	<b>-6.55</b>	-1.24	-1.63	-3.65	<b>-4.72</b>

TABLE IV  
PERFORMANCE COMPARISON OF DIFFERENT PRE-FILTER METHODS ACROSS VARIOUS ENCODERS ON HEVC-B.

Encoder	Method	PSNR	PSNR-HVSM	MS-SSIM	VMAF-NEG	ALL
libaom	Ours	<b>-0.34</b>	<b>-5.70</b>	<b>-4.71</b>	<b>-6.20</b>	<b>-4.24</b>
	[9]	0.67	-3.26	-3.49	-3.29	-2.34
	[6]	1.42	-3.25	-2.14	-1.48	-1.36
	[5]	1.30	-2.43	-1.26	0.66	-0.43
	Ours	<b>0.00</b>	<b>-6.81</b>	<b>-4.47</b>	<b>-5.66</b>	<b>-4.23</b>
x265	[9]	1.01	-3.85	-3.31	-2.67	-2.21
	[6]	2.04	-5.15	-2.69	-1.48	-1.82
	[5]	0.58	-3.98	-2.44	0.05	-1.45
	Ours	<b>-1.51</b>	<b>-7.17</b>	<b>-5.93</b>	<b>-5.60</b>	<b>-5.05</b>
x264	[9]	0.10	-4.06	-4.31	-3.00	-2.82
	[6]	-0.52	-6.55	-4.86	-2.45	-3.60
	[5]	<b>-2.00</b>	-5.93	-4.90	-1.55	-3.59
	Ours	<b>-1.51</b>	<b>-7.17</b>	<b>-5.93</b>	<b>-5.60</b>	<b>-5.05</b>

#### IV. EXPERIMENTS

##### A. Experimental Setup

All experiments are conducted using our FJNDF-Pytorch benchmark under the All-Intra configuration with QP values {27, 32, 37, 42}, measuring BD-BR [10] savings (%). We evaluate our method against three state-of-the-art pre-filters [5], [6], [9] on four encoders [20]–[23] and datasets [14]–[17], as detailed in Table I. In line with the competing methods, we process only the luma channel in all experiments.

For training, we use the Adam optimizer for 100K iterations with a batch size of 16 on 224x224 patches and an initial learning rate of 3e-4. The loss weights ( $\lambda_1, \lambda_2$  and  $\lambda_3$ ) for  $L_c$ ,  $L_m$ , and  $L_{freq}$  are set to 1.0, 0.16, and 0.02, respectively, with a zigzag cutoff  $K = 10$  for  $L_{det}^{cons}$ .

##### B. Experimental Results

As shown in Table III, our method consistently outperforms both state-of-the-art competitors on the VVenC encoder across all datasets. For instance, on the HEVC-B dataset, our approach achieves a remarkable -4.84% BD-BR saving in VMAF. Furthermore, our approach demonstrates its robustness by securing the highest overall performance on all four datasets, with BD-BR savings ranging from -2.80% to -4.72%.

To validate its generalizability, we conduct further comparisons on HEVC-B across libaom, x265, and x264 encoders. Table IV confirm that our method consistently achieves the best overall performance across all tested encoders, with significant gains of -4.24%, -4.23%, and -5.05%, respectively. This highlights the robustness and wide applicability of our approach.

Due to space constraints, we cannot present the full results for all combinations of datasets and encoders in this paper. However, these comprehensive results are documented and available in our benchmark for reference.

TABLE V  
ABLATION STUDY OF DIFFERENT COMPONENTS OF HEVC-B ON VVENC.

Method	PSNR	PSNR-HVSM	MS-SSIM	VMAF-NEG	ALL
Reference	1.95	-2.75	-1.35	-0.67	-0.70
BaseLine	3.52	-5.50	-3.50	-2.85	-2.08
BaseLine + $L_{freq}$	0.69	-4.43	-3.34	-4.18	-2.81
Ours (Lightweight)	0.87	-4.20	-2.90	-3.67	-2.47

TABLE VI  
MODEL SIZE, COMPUTATIONAL COST, AND INFERENCE LATENCY.

Method	Parameters (K)		GFLOPs	Inference Time	
	Train	Inference		CPU <sup>a</sup> (s)	GPU <sup>b</sup> (ms)
[5]	/	/	/	~ 70	/
[6]	/	/	/	~ 20	/
[9]	<b>12.23</b>	12.22	50.70	0.835	15.43
BaseLine	38.92	3.06	12.15	0.595	13.04
Ours	24.95	<b>1.86</b>	<b>7.15</b>	<b>0.428</b>	<b>10.88</b>

<sup>a</sup>Intel(R) Xeon(R) Gold 6230 CPU. <sup>b</sup>NVIDIA GeForce RTX 2080 Ti GPU.

##### C. Ablation Study

We conduct ablation studies to validate our key contributions, with results in Table V. The *Baseline* model, trained with only spatial-domain loss, surpasses the *Reference* in perceptual metrics but degrades PSNR. The introduction of our proposed loss,  $L_{freq}$ , not only rectifies the PSNR degradation, but also boosts perceptual performance in VMAF, confirming the effectiveness of our frequency-domain loss.

Table V also shows that our final lightweight model, compared to the baseline model, retains the majority of the perceptual optimization capability while operating at a significantly lower computational cost. As detailed in Table VI, our final model requires only 7.15 GFLOPs and 1.86K parameters. In addition, we tested the inference time for different methods on both CPU and GPU platform. Methods [5], [6] are our re-implementations, and the measured times are comparable to those reported in [6]. These results validate that our network design is state-of-the-art in both efficiency and effectiveness.

#### V. CONCLUSION

In this paper, we propose a learning framework for a lightweight JND-guided pre-filter network. The core of our method is a novel frequency-domain loss that references the original input signal to correct the inherent flaws of its training target. Our resulting model achieves a new state-of-the-art balance between compression efficiency and computational cost, demonstrating superiority across multiple encoders. The open-sourced FJNDF-Pytorch platform provides a solid foundation for these contributions and for future research in this area. Building on this work, we plan to expand our benchmark to comprehensively evaluate a wider array of methods, including spatial, temporal, and other learning-based approaches.

## REFERENCES

- [1] L. Ding, G. Li, R. Wang, and W. Wang, "Video pre-processing with jnd-based gaussian filtering of superpixels," in *Visual Information Processing and Communication VI*, vol. 9410. SPIE, 2015, pp. 20–25. 1
- [2] E. Vidal, N. Sturmel, C. Guillemot, P. Corlay, and F.-X. Coudoux, "New adaptive filters as perceptual preprocessing for rate-quality performance optimization of video coding," *Signal Processing: Image Communication*, vol. 52, pp. 124–137, 2017. 1
- [3] X. Luo, J. Huang, G. Xiang, H. Fan, Y. Hou, and W. Yan, "Recursively adaptive perceptual non-local means for video coding," in *Thirteenth International Conference on Digital Image Processing (ICDIP 2021)*, vol. 11878. SPIE, 2021, pp. 455–462. 1
- [4] S. Ki, M. Kim, and H. Ko, "Just-noticeable-quantization-distortion based preprocessing for perceptual video coding," in *2017 IEEE Visual Communications and Image Processing (VCIP)*. IEEE, 2017, pp. 1–4. 1
- [5] B. Kang and W. Kim, "Human perception-oriented enhancement and smoothing for perceptual video coding," *IEEE Transactions on Broadcasting*, vol. 69, no. 3, pp. 767–778, 2023. 1, 2, 4
- [6] H. Tan, G. Xiang, X. Xie, and H. Jia, "Joint frame-level and block-level rate-perception optimized preprocessing for video coding," in *Proceedings of the 6th ACM International Conference on Multimedia in Asia*, 2024, pp. 1–1. 1, 2, 3, 4
- [7] G. Xiang, H. Jia, J. Liu, B. Cai, Y. Li, and X. Xie, "Adaptive perceptual preprocessing for video coding," in *2016 IEEE International Symposium on Circuits and Systems (ISCAS)*. IEEE, 2016, pp. 2535–2538. 1, 2
- [8] S. Ki, J. Do, and M. Kim, "Learning-based jnd-directed hdr video preprocessing for perceptually lossless compression with hevcc," *IEEE Access*, vol. 8, pp. 228 605–228 618, 2020. 1
- [9] Y.-H. Sun, C. L.-H. Lee, and T.-S. Chang, "Iqnet: Image quality assessment guided just noticeable difference prefiltering for versatile video coding," *IEEE Open Journal of Circuits and Systems*, vol. 5, pp. 17–27, 2023. 1, 4
- [10] G. Bjontegaard, "Calculation of average PSNR differences between RD-curves," *ITU SG16 Doc. VCEG-M33*, 2001. 1, 4
- [11] Z. Wei and K. N. Ngan, "Spatio-temporal just noticeable distortion profile for grey scale image/video in dct domain," *IEEE Transactions on Circuits and Systems for Video Technology*, vol. 19, no. 3, pp. 337–346, 2009. 2
- [12] S.-H. Bae and M. Kim, "A novel dct-based jnd model for luminance adaptation effect in dct frequency," *IEEE Signal Processing Letters*, vol. 20, no. 9, pp. 893–896, 2013. 2
- [13] S.-H. Bae, J. Kim, and M. Kim, "Hevc-based perceptually adaptive video coding using a dct-based local distortion detection probability model," *IEEE Transactions on Image Processing*, vol. 25, no. 7, pp. 3343–3357, 2016. 2, 3
- [14] F. Bossen, "Common test conditions and software reference configurations," in *3rd. JCT-VC Meeting, Guangzhou, CN, October 2010*, 2010. 2, 4
- [15] Xiph.Org Foundation, "Xiph.org video test media (derf's collection)," <https://media.xiph.org/video/derf/>, 2013, accessed on: 2025-09-30. 2, 4
- [16] H. Wang, W. Gan, S. Hu, J. Y. Lin, L. Jin, L. Song, P. Wang, I. Katsavounidis, A. Aaron, and C.-C. J. Kuo, "Mcl-jcv: a jnd-based h.264/avc video quality assessment dataset," in *2016 IEEE international conference on image processing (ICIP)*. IEEE, 2016, pp. 1509–1513. 2, 4
- [17] L. Jin, J. Y. Lin, S. Hu, H. Wang, P. Wang, I. Katsavounidis, A. Aaron, and C.-C. J. Kuo, "Statistical study on perceived jpeg image quality via mcl-jci dataset construction and analysis," *Electronic Imaging*, vol. 2016, no. 13, pp. 1–9, 2016. 2, 4
- [18] E. Agustsson and R. Timofte, "Ntire 2017 challenge on single image super-resolution: Dataset and study," in *Proceedings of the IEEE conference on computer vision and pattern recognition workshops*, 2017, pp. 126–135. 2, 3
- [19] H. Lin, G. Chen, M. Jenadeleh, V. Hosu, U.-D. Reips, R. Hamzaoui, and D. Saupe, "Large-scale crowdsourced subjective assessment of picturewise just noticeable difference," *IEEE Transactions on Circuits and Systems for Video Technology*, 2022. 2, 3
- [20] VideoLAN Project, "x264: A high-performance h.264/avc encoder," <https://www.videolan.org/developers/x264.html>, 2024, accessed on: 2025-09-30. 2, 4
- [21] MulticoreWare, Inc., "x265: An open-source hevcc encoder library," <https://x265.org/>, 2025, accessed on: 2025-10-26. 2, 4
- [22] Alliance for Open Media (AOMedia), "libaom: Av1 codec library," <https://aomedia.org/>, 2024, accessed on: 2025-09-30. 2, 4
- [23] A. Wiecekowski, J. Brandenburg, T. Hinz, C. Bartnik, V. George, G. Hege, C. Helmrich, A. Henkel, C. Lehmann, C. Stoffers *et al.*, "Vvenc: An open and optimized vvc encoder implementation," in *2021 IEEE International Conference on Multimedia & Expo Workshops (ICMEW)*. IEEE, 2021, pp. 1–2. 2, 4
- [24] N. Ponomarenko, F. Silvestri, K. Egiazarian, M. Carli, J. Astola, and V. Lukin, "On between-coefficient contrast masking of dct basis functions," in *Proceedings of the third international workshop on video processing and quality metrics*, vol. 4. Scottsdale USA, 2007. 2
- [25] Z. Wang, A. C. Bovik, H. R. Sheikh, and E. P. Simoncelli, "Image quality assessment: from error visibility to structural similarity," *IEEE transactions on image processing*, vol. 13, no. 4, pp. 600–612, 2004. 2
- [26] Z. Wang, E. P. Simoncelli, and A. C. Bovik, "Multiscale structural similarity for image quality assessment," in *The thirty-seventh asilomar conference on signals, systems & computers*, 2003, vol. 2. Ieee, 2003, pp. 1398–1402. 2
- [27] Z. Li, A. Aaron, I. Katsavounidis, A. Moorthy, and M. Manohara, "Toward a practical perceptual video quality metric," <https://netflixtechblog.com/toward-a-practical-perceptual-video-quality-metric-653f208b9652>, 2016, accessed on: 2025-09-30. 2
- [28] A. Zvezdakova, S. Zvezdakov, D. Kulikov, and D. Vatolin, "Hacking vmaf with video color and contrast distortion," *arXiv preprint arXiv:1907.04807*, 2019. 2
- [29] P. Charbonnier, L. Blanc-Feraud, G. Aubert, and M. Barlaud, "Two deterministic half-quadratic regularization algorithms for computed imaging," in *Proceedings of 1st international conference on image processing*, vol. 2. IEEE, 1994, pp. 168–172. 2, 3
- [30] J. Snell, K. Ridgeway, R. Liao, B. D. Roads, M. C. Mozer, and R. S. Zemel, "Learning to generate images with perceptual similarity metrics," in *2017 IEEE international conference on image processing (ICIP)*. IEEE, 2017, pp. 4277–4281. 2, 3
- [31] C. Chen and J. Mo, "IQA-PyTorch: Pytorch toolbox for image quality assessment," [Online]. Available: <https://github.com/chaofengc/IQA-PyTorch>, 2022. 2
- [32] X. Wang, L. Xie, K. Yu, K. C. Chan, C. C. Loy, and C. Dong, "BasicSR: Open source image and video restoration toolbox," <https://github.com/XPixelGroup/BasicSR>, 2022. 2
- [33] H. Yan, A. Li, X. Zhang, Z. Liu, Z. Shi, C. Zhu, and L. Zhang, "Mobileie: An extremely lightweight and effective convnet for real-time image enhancement on mobile devices," *arXiv preprint arXiv:2507.01838*, 2025. 3